



# Thermal analysis study of $\text{LiFeO}_2$ formation from $\text{Li}_2\text{CO}_3\text{--Fe}_2\text{O}_3$ mechanically activated reagents

Elena N. Lysenko<sup>1</sup> · Anatoly P. Surzhikov<sup>1</sup> · Evgeniy V. Nikolaev<sup>1</sup> · Vitaly A. Vlasov<sup>1</sup>

Received: 31 October 2017 / Accepted: 23 February 2018 / Published online: 5 March 2018  
© Akadémiai Kiadó, Budapest, Hungary 2018

## Abstract

The solid-phase synthesis of  $\text{LiFeO}_2$  lithium ferrite from mechanically activated  $\text{Fe}_2\text{O}_3\text{--Li}_2\text{CO}_3$  initial reagent mixtures was investigated by X-ray powder diffraction and thermal analysis techniques. The mechanical milling of powder mixture was carried out by AGO-2S planetary ball mill with a rotation speed of 2220 rpm for 60 min. According to the XRD data, the crystallite sizes of milled reagents decrease as a result of ball milling. From thermal analysis, it was shown that the ferrite synthesis starts with the interaction between reagents and lithium carbonate decomposition and accompanied by mass loss process due to  $\text{CO}_2$  evaporation. For non-milled mixtures, the mass loss process occurs in the temperature range 400–740 °C and comprises two steps. As for milled samples, this process shifts toward lower temperatures, where a slight mass loss process is observed from 100 °C up to 400 °C, while the main mass loss occurs in the temperature range of 400–550 °C in one stage. The results indicate that the major mechanism of solid-state reaction can be attributed to the two-step model of the reaction proceed, whose rate is diffusion controlled over the entire temperature range for non-milled mixture, but corresponds to the diffusion and  $n$ -order equation depending on conversion degree for milled mixture. Generally, a preliminary mechanical activation of  $\text{Fe}_2\text{O}_3\text{--Li}_2\text{CO}_3$  considerably enhances the reactivity of the solid-phase system, thereby reducing the temperature of lithium ferrite thermal synthesis. Thus,  $\text{LiFeO}_2$  ferrite can be obtained from reagents mixture mechanically activated for 60 min at temperature of 600 °C for 2 h, that is, at a significantly lower synthesis time and temperature than in the case of using conventional solid-state synthesis from non-milled reagents.

**Keywords** Lithium ferrites ·  $\text{LiFeO}_2$  · Solid-phase synthesis · Mechanical activation · Ball milling · Thermal analysis · TG/DSC

## Introduction

Lithium ferrite,  $\text{LiFeO}_2$ , has attracted considerable interest due to its potential industrial applications, for example, as a cathode material in lithium rechargeable batteries because it has lower toxicity and cost, relative to  $\text{LiNiO}_2$  and  $\text{LiCoO}_2$  [1–3]. In most of cases, it is necessary to obtain a nanostructured  $\text{LiFeO}_2$ , which can be achieved by using lower synthesis temperatures.

The solid-state synthesis is the main method of lithium ferrites production, which has a tendency to yield coarse-grained agglomerated powders with compositional

inhomogeneities. Therefore, the conventional method requires a high synthesis temperature and a long time to manufacture ferrites with homogeneous composition [4–7].

The new low-temperature methods of lithium ferrites synthesis have received attention in recent years such as coprecipitation, sol–gel synthesis, hydrothermal reactions and citrate routes [8–11]. However, for these synthesis procedures, high-purity inorganic or organometallic chemicals have to be employed as starting materials, which are more expensive than the widely available oxides and carbonates.

It is known that one way to prepare powdered materials in a highly dispersed state and with disordered structure is the use of the mechanical activation in high-energy ball mills [12–14]. Mechanically activated ferrite powders are highly reactive, and therefore, the final products at lower

✉ Evgeniy V. Nikolaev  
nikolaev0712@gmail.com

<sup>1</sup> Tomsk Polytechnic University, Tomsk, Russia

temperatures and durations of thermal treatment could be obtained.

According to earlier investigations, mechanical activation can be used to produce lithium and substituted lithium ferrites at lower temperature than in conventional ceramic processing [15–19]. However, for these studies, mechanical activation was accomplished in a high-energy ball mills at low rotation speeds of 200–450 rpm using a long activation time. In our previous works [20, 21], the formations of  $\text{LiFe}_5\text{O}_8$ ,  $\text{LiZn}$  and  $\text{LiTi}$  ferrites from reagents mixtures, which were mechanically activated in a high-energy planetary ball mill with a rotation speed of 2220 rpm, were studied.

In this work, the effect of 2220-rpm mechanical activation of  $\text{Fe}_2\text{O}_3$ – $\text{Li}_2\text{CO}_3$  initial reagents on  $\text{LiFeO}_2$  synthesis was investigated by X-ray diffraction (XRD), thermogravimetric (TG/DTG) and calorimetric (DSC) analysis.

## Experimental

The initial reagents were commercially  $\text{Fe}_2\text{O}_3$  and  $\text{Li}_2\text{CO}_3$  powders which were pre-dried and weighed in molar ratios according to the equation  $\text{Li}_2\text{CO}_3 + \text{Fe}_2\text{O}_3 \rightarrow 2\text{LiFeO}_2 + \text{CO}_2\uparrow$ .

The mixture was divided into two batches; the samples of first batch were simply mixed in an agate mortar and are considered to be simple physical mixtures (non-milled samples). The samples from the second batch were mechanically activated using AGO-2S (Novic, Russia) high-energy planetary ball mill with stainless steel balls and vials for 60 min (milled samples). The weights of the material and balls were in the ratio 1:10. The milling was performed in the dry state at 2220 rpm rotation speed for vial (centrifugal acceleration  $g = 100$ ) and stopped for 5 min for every 15 min of milling to cool down the system.

TG/DSC measurements were taken by simultaneous thermal analyzer STA 449C Jupiter (Netzsch-Gerätebau GmbH) in a non-isothermal mode in air with different heating rates of 2.5, 5, 10, 20  $^\circ\text{C min}^{-1}$  and a temperature range of 20–900 $^\circ\text{C}$ . Both TG and DSC baselines were corrected by the subtraction of predetermined baselines run under identical conditions except for the absence of sample. Mass spectrometer QMS 403C was used for qualitative mass spectrometry (MS) analysis of the evolved gases during heating of the samples. The Netzsch Proteus software packages were used for data analysis.

Additionally, the model-fitting kinetic analysis of ferrite formation was performed by using full TG data (mass change at different heating rates) and Netzsch Thermokinetics software where both the model free by Friedman

analysis and the nonlinear regression model-fitting analysis were used.

Phase compositions of ferrite were determined by X-ray diffraction analysis using ARL X'TRA diffractometer with  $\text{CuK}\alpha$  radiation. The Powder Cell 2.4 software was used for a full-profile analysis of XRD patterns.

## Results and discussion

Figure 1 shows XRD patterns for  $\alpha$ - $\text{Fe}_2\text{O}_3$  (PDF No. 40-142) and  $\text{Li}_2\text{CO}_3$  (PDF No. 66-941) initial reagents. Figures 2 and 3 show the X-ray diffraction patterns for non-milled mixture (Fig. 2) and milled mixture (Fig. 3). The structural parameters and crystallite sizes were examined from XRD analysis, and these data are summarized in Table 1.

The XRD data for non-milled  $\text{Li}_2\text{CO}_3$ – $\text{Fe}_2\text{O}_3$  mixture (Fig. 2) indicate the presence of  $\alpha$ - $\text{Fe}_2\text{O}_3$  and  $\text{Li}_2\text{CO}_3$  phases (marked reflections). For the mechanically activated mixture (Fig. 3), a decrease in the intensities and an increase in the half width of reflections were observed as a result of particle milling. Regardless of ball milling, X-ray absorption coefficients for  $\text{Li}_2\text{CO}_3$  and  $\text{Fe}_2\text{O}_3$  are very different. Thus, after milling, the intensity of the reflections for  $\text{Li}_2\text{CO}_3$  decreases more strongly than for iron oxide.

The crystallite size (coherent length) of the  $\alpha$ - $\text{Fe}_2\text{O}_3$  phase determined by the Williamson-Hall method from XRD data decreased after milling for 60 min. However, one can notice an increase in the lattice parameters for both reagents.

Figures 4 and 5 show the TG/DTG/DSC and MS curves for the non-milled (Fig. 4) and milled for 60 min (Fig. 5)  $\text{Li}_2\text{CO}_3$ – $\text{Fe}_2\text{O}_3$  mixtures. From Fig. 4a, it can be seen that the mass loss process occurs in temperature range of 400–740  $^\circ\text{C}$ , which comprises two steps corresponding to the interaction between reagents and the decomposition of

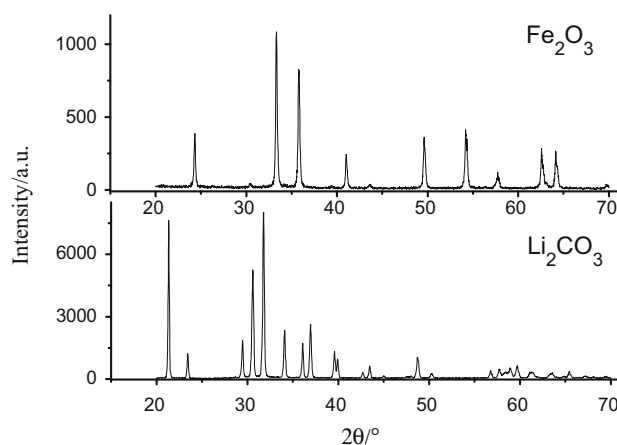
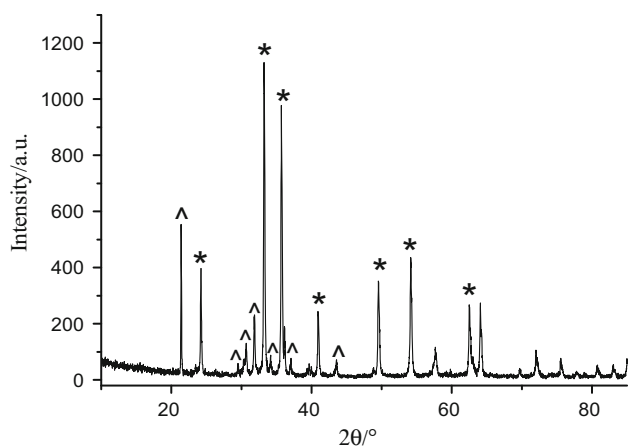
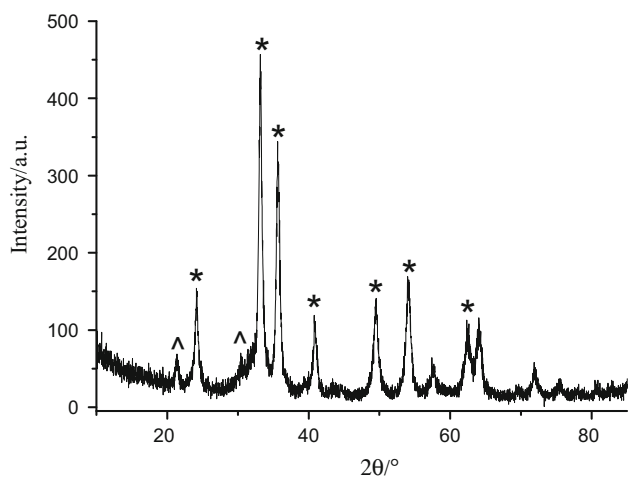


Fig. 1 XRD patterns for initial reagents



**Fig. 2** XRD pattern for non-milled Li<sub>2</sub>CO<sub>3</sub>-Fe<sub>2</sub>O<sub>3</sub> mixture (\*—Fe<sub>2</sub>O<sub>3</sub>, ^—Li<sub>2</sub>CO<sub>3</sub>)



**Fig. 3** XRD pattern for milled Li<sub>2</sub>CO<sub>3</sub>-Fe<sub>2</sub>O<sub>3</sub> mixture (\*—Fe<sub>2</sub>O<sub>3</sub>, ^—Li<sub>2</sub>CO<sub>3</sub>)

the unreacted portion of lithium carbonate at 726 °C [4]. In this temperature range, the DSC curve shows a wide endothermic peak. The shape of the DTG curve is similar to the DSC curve, which shows that the mass change in this temperature range can be attributed to the observed endothermic effect. According to the mass spectrometry analysis of gases (Fig. 4b), only CO<sub>2</sub> is released during the reaction. The mean total mass loss was (18.9 ± 0.1) %, and this value corresponds to the value calculated as the

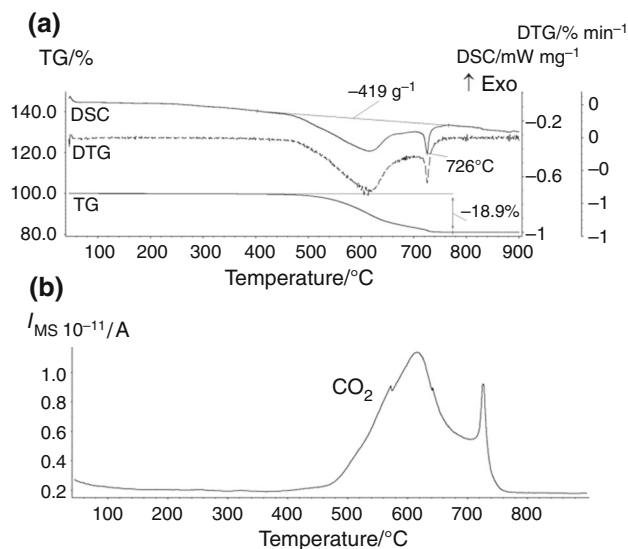


**Fig. 4** TG/DTG/DSC (a), mass spectrometric (b) curves for non-milled Li<sub>2</sub>CO<sub>3</sub>-Fe<sub>2</sub>O<sub>3</sub> mixture

mass loss of the process  $\text{Li}_2\text{CO}_3 + \text{Fe}_2\text{O}_3 \rightarrow 2\text{LiFeO}_2 + \text{CO}_2$ .

As for mechanically activated mixture (Fig. 5a), the mass loss process shifts toward lower temperatures. A slight mass loss process was observed on TG curve from 100 °C up to 400 °C, while the main mass loss occurs in the temperature range of 400–550 °C in one stage, where a narrow DSC peak is observed. It has to be noted that this mass loss is completed at a temperature well below that where spontaneous decomposition of Li<sub>2</sub>CO<sub>3</sub> occurs. In this case the mean total mass loss also corresponds to the calculated value for CO<sub>2</sub> evaporation (Fig. 5b).

The DSC peak shows an endothermic peak with an enthalpy of 389 J g<sup>-1</sup>, while the DSC measurement for non-milled mixture resulted in an endothermic peak with an enthalpy of 419 J g<sup>-1</sup>. If it is assumed that the 30 J g<sup>-1</sup> difference in enthalpy is due to slow ferrite formation at lower temperatures, then ca. 7.2% was formed below 400 °C.

As known [22, 23], the kinetic analysis is based on the experimental determination of degree or rate of conversion depending on the reaction conditions and the mathematical description of the found dependence as well as the

**Table 1** XRD data for investigated samples

Sample	Phase	Lattice parameter/Å	Crystallite size/nm
Non-milled mixture	Fe <sub>2</sub> O <sub>3</sub>	$a = b = 5.035; c = 13.752$	99
	Li <sub>2</sub> CO <sub>3</sub>	$a = 8.384, b = 4.973, c = 6.205$	78
Milled mixture	Fe <sub>2</sub> O <sub>3</sub>	$a = b = 5.037; c = 13.760$	24
	Li <sub>2</sub> CO <sub>3</sub>	$a = 8.388, b = 4.993, c = 6.222$	20
Ferrite	LiFeO <sub>2</sub>	$a = b = c = 4.158$	124

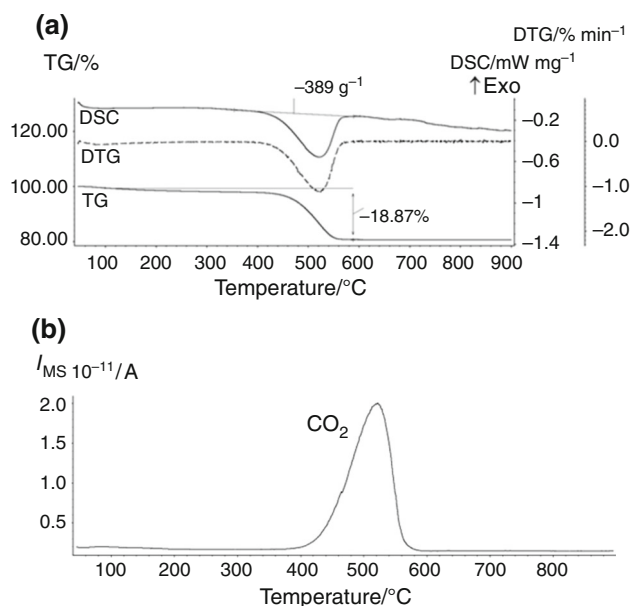


**Fig. 5** TG/DTG/DSC (a), mass spectrometric (b) curves for milled  $\text{Li}_2\text{CO}_3\text{-Fe}_2\text{O}_3$  mixture

evaluation of kinetic parameters of the reaction and their interpretation in relation with the nature of processes.

The equation used for kinetic analysis is:

$$da/dt = k(T)f(a) = k_0f(a) \exp(-E_a/RT) \quad (1)$$

where  $\alpha$  is conversion degree,  $da/dt$  is a linear function of a temperature-dependent rate constant  $k(T)$ ,  $f(\alpha)$  is a temperature-independent function of the conversion ratio,  $k_0$  is the pre-exponential factor,  $E_a$  is the activation energy,  $T$  is the absolute temperature, and  $R$  is the gas constant.

The above equation may be extended to describe complex processes such as concurrent or consecutive reactions, each with its own kinetic parameters. The reaction models  $f(\alpha)$ , most commonly used in heterogeneous kinetics, are presented somewhere else [22].

The aim of this model-fitting kinetic approach is to find a kinetic model with minimal adjustable parameters which quantitatively describes the kinetics reaction [23–25]. This formal kinetic model can then be used for the kinetic analysis of thermal measurements, including the process of synthesis [26].

A model-free isoconversion method of the Friedman analysis [27] available in the thermokinetics software was used for an initial estimate of the kinetic parameters. Results from the Friedman analysis are presented in Fig. 6 for non-milled mixture and in Fig. 7 for milled  $\text{Li}_2\text{CO}_3\text{-Fe}_2\text{O}_3$  mixture. These results include isoconversion lines in pre-exponential plots (Figs. 6a, 7a) and Arrhenius parameters (pre-exponential factor and activation energy) which are the strong functions of the conversion ratio  $\alpha$  (Figs. 6b, 7b).

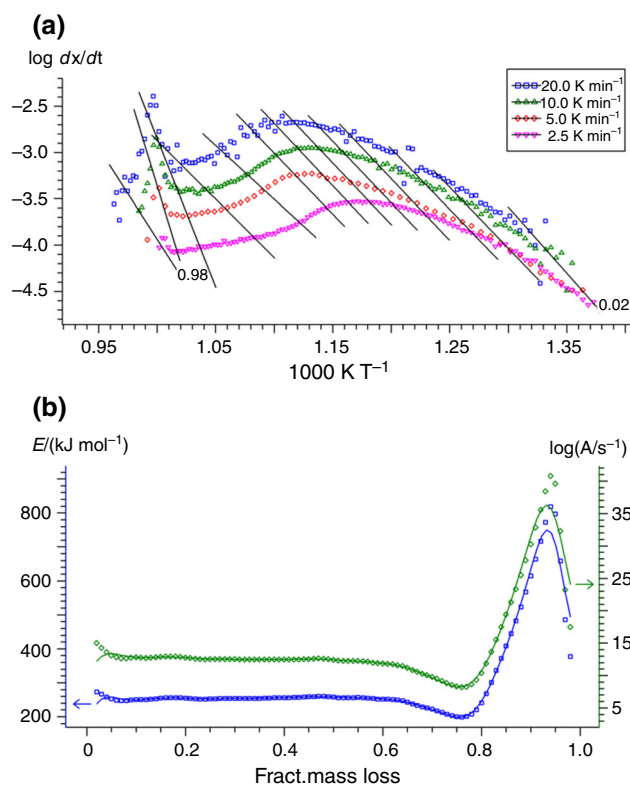


**Fig. 6** Arrhenius parameters derived from the Friedman analysis for non-milled  $\text{Li}_2\text{CO}_3\text{-Fe}_2\text{O}_3$  mixture

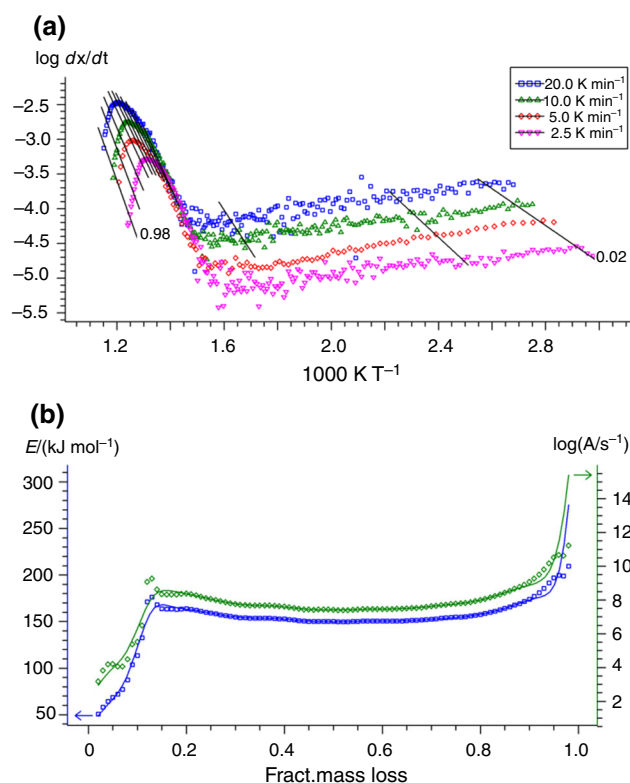


**Fig. 7** Arrhenius parameters derived from the Friedman analysis for milled  $\text{Li}_2\text{CO}_3\text{-Fe}_2\text{O}_3$  mixture

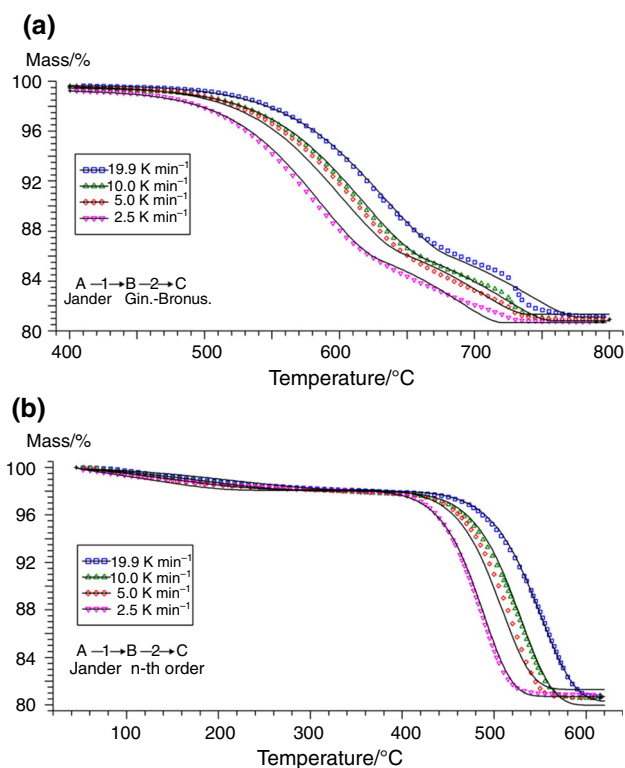


**Fig. 8** Fit for nonlinear regression of the TG kinetic data of non-milled (a), milled (b) Li<sub>2</sub>CO<sub>3</sub>-Fe<sub>2</sub>O<sub>3</sub> mixture (symbols—experimental points, lines—calculated curves)

From Figs. 6a and 7a the experimental points at the start of the reaction ( $0.02 \leq \alpha \leq 0.1$ ) show a lower slope than the isoconversion lines in pre-exponential plots for both mixtures, and it should deal with a diffusion reaction. Generally, the diffusion-controlled processes are characterized by low activation energies. We can assume that the initial stage of ferrite synthesis is likely to be diffusion-controlled.

The behavior of the  $E_a$  curves (Figs. 6b, 7b) for both mixtures indicates the existence of a two-step model (A → B → C) of the reaction proceeds with different Arrhenius parameters. However, the transition from one stage to another for non-milled mixture occurs at  $\alpha \sim 0.6$  as compared to the milled samples, where the first step is observed in the  $\alpha$  range from 0 to 0.15.

From Friedman analysis, the pre-exponential factors and the activation energies were used as input values for the nonlinear regression model-fitting procedure.

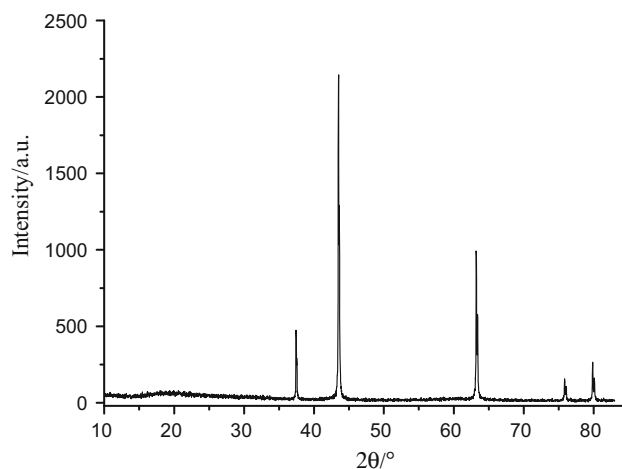


**Fig. 9** XRD pattern for LiFeO<sub>2</sub> ferrite

By the model of nonlinear regression, the fitting of the TG data obtained at different heating rates was produced by the several kinetic models: Yander, Ginstling-Brounshtein, Abraham-Erofeev, etc. Figure 8 shows the results from the nonlinear regression analysis for both mixtures, which are summarized in Table 2.

For non-milled mixture (Fig. 8a), the best results were obtained using in the first stage the diffusion model of Yander and the diffusion model of Ginstling-Brounshtein in the second stage. One can observe that the activation energies obtained from both models are very close. These values appear to be high and might be caused by a difficult decomposition of lithium carbonate.

As for milled mixture (Fig. 8b), the best fitting two-step mechanism employed the Yander model and  $n$ -order equation for the first and second steps, respectively. According to the results, the lower values of the activation energy are observed compared to non-milled mixture.  $E_a$  in the first stage has a low value and then increases in the second stage. It should be noted that the full reaction of the first stage is shifted to lower values  $\alpha$ , as shown in the last column of Table 2. This result is consistent with Friedman analysis.

Figure 9 shows X-ray diffraction pattern for LiFeO<sub>2</sub> ferrite, which was synthesized at 600 °C during 120 min via isothermal heating in thermal analyzer. The reflections belong to the  $\alpha$ -LiFeO<sub>2</sub> ferrite and indicate the high level of phase homogeneity of lithium ferrite. One can notice that this regime allows obtaining the  $\alpha$ -LiFeO<sub>2</sub> ferrite at a significantly lower synthesis time and temperature than in

**Table 2** Kinetic results derived from nonlinear regression analysis

Mixture	$\log A_1/s^{-1}$	$E_{a1}/kJ\ mol^{-1}$	$\log A_2/s^{-1}$	$E_{a2}/kJ\ mol^{-1}$	$n_2$	FollReact. $2/\alpha$
Non-milled	12.8	271	12.8	304	—	0.67
Milled	0.14	33	8.1	160	1.01	0.10

the case of using conventional solid-state synthesis from non-milled reagents [5, 16].

Given the nature of mechanical milling, the results suggest that high surface area particles of  $\alpha$ -Fe<sub>2</sub>O<sub>3</sub> and Li<sub>2</sub>CO<sub>3</sub> are formed by milling for 60 min and it would be reasonable to expect these particles to be tightly pressed together with a large interface between the reactant particles. This effect, according to thermal analysis, leads to increasing the reactivity of the solid-state system, which is to lower the temperature of LiFeO<sub>2</sub> synthesis.

## Conclusions

The solid-phase synthesis of LiFeO<sub>2</sub> lithium ferrite from mechanically activated Fe<sub>2</sub>O<sub>3</sub>–Li<sub>2</sub>CO<sub>3</sub> initial reagent mixtures was investigated by X-ray powder diffraction and thermal analysis techniques.

It was established that the mechanical activation of Fe<sub>2</sub>O<sub>3</sub>–Li<sub>2</sub>CO<sub>3</sub> mixture considerably enhanced the reactivity of the solid system, thereby reducing the temperature of lithium ferrite synthesis. Thus, LiFeO<sub>2</sub> ferrite can be obtained from reagents mechanically activated for 60 min at temperature of 600 °C for 2 h, that is, at a significantly lower synthesis time and temperature than in the case of using conventional solid-state synthesis from non-milled reagents. The results obtained are consistent with earlier results for lithium-substituted ferrites formation from mechanically activated initial reagents [15].

The results indicate that the major mechanism of solid-state reaction can be attributed to the two-step model of the reaction proceed, whose rate is diffusion controlled over the entire temperature range for non-milled mixture, but corresponds to diffusion and  $n$ -order equation depending on conversion degree for milled mixture. Technically, the obtained data are very valuable for the control and optimization of synthesis processes, which is an important issue for the further use of ferrite powders.

**Acknowledgements** This work was supported by the Ministry of Education and Science of the Russian Federation in part of the Science Program (Project 11.980.2017/4.6). The experiments on equipments and participation in scientific conference were funded from Tomsk Polytechnic University Competitiveness Enhancement Program Grant.

## References

- Sakurai Y, Arai H, Okada S, Yamaki J. Low temperature synthesis and electrochemical characterization of LiFeO<sub>2</sub> cathodes. *J Power Sources*. 1997;68:711–5.
- Dahn JR, Von Sacken U, Michal CA. Structure and electrochemistry of Li<sub>1 ± y</sub>NiO<sub>2</sub> and a new Li<sub>2</sub>NiO<sub>2</sub> phase with the Ni(OH)<sub>2</sub> structure. *Solid State Ion*. 1990;44:87–97.
- Sakurai Y, Arai H, Yamaki J. Preparation of electrochemically active  $\alpha$ -LiFeO<sub>2</sub> at low temperature. *Solid State Ion*. 1998;113–115:29.
- El-Shobaky GA, Ibrahim AA. Solid-solid interactions between ferric oxide and lithium carbonate and the thermal stability of the lithium ferrites produced. *Thermochim Acta*. 1987;118:151–8.
- Rakshit SK, Parida SC, Naik YP, Venugopal V. Thermodynamic studies on lithium ferrites. *J Solid State Chem*. 2011;184:1186–94.
- Surzhikov AP, Pritulov AM, Lysenko EN, Vlasov VA, Vasendina EA, Malyshev AV. Analysis of the phase composition and homogeneity of ferrite lithium-substituted powders by the thermomagnetometry method. *J Therm Anal Calorim*. 2013;112:739–45.
- Teixeira SS, Graça MPF, Costa LC. Dielectric, morphological and structural properties of lithium ferrite powders prepared by solid state method. *J Noncryst Solids*. 2012;358:1924–9.
- Randhawa BS, Dosanjh HS, Kumar N. Synthesis of lithium ferrite by precursor and combustion methods: a comparative study. *J Radioanal Nucl Chem*. 2007;274:581–91.
- Verma V, Pandey V, Aloysius RP, Annapoomi S, Kotanala RK. Comparative study of structural and magnetic properties of nanocrystalline Li<sub>0.5</sub>Fe<sub>2.5</sub>O<sub>4</sub> prepared by various methods. *Phys B*. 2009;404:2309–14.
- Aravind G, Raghasudha M, Ravinder DM, Manivel R, Meena SS, Bhatt P. Study of structural and magnetic properties of Li–Ni nanoferrites synthesized by citrate-gel auto combustion method. *Ceram Int*. 2016;42:2941–50.
- Tabuchi M, Ado K, Sakaebe H, Masquelier C, Kageyama H, Nakamura O. Preparation of AFeO<sub>2</sub> (A = Li, Na) by hydrothermal method. *Solid State Ion*. 1995;79:220.
- Berbenni V, Bruni G, Milanese C, Girella A, Marini A. Synthesis and characterization of LaFeO<sub>3</sub> powders prepared by a mixed mechanical/thermal processing route. *J Therm Anal Calorim*. 2017. <https://doi.org/10.1007/s10973-017-6878-z>.
- Parlak TT, Apaydin F, Yildiz K. Formation of SrTiO<sub>3</sub> in mechanically activated SrCO<sub>3</sub>–TiO<sub>2</sub> system. *J Therm Anal Calorim*. 2017;127:63–9.
- Mihalache V. Thermal analysis of ball-milled Fe–14Cr–3 W–0.4Ti–0.25Y<sub>2</sub>O<sub>3</sub> ferritic steel powder. *J Therm Anal Calorim*. 2016;124:1179–92.
- Berbenni V, Marini A, Matteazzi P, Ricceri R, Welham NJ. Solid-state formation of lithium ferrites from mechanically activated Li<sub>2</sub>CO<sub>3</sub>–Fe<sub>2</sub>O<sub>3</sub> mixtures. *J Eur Ceram Soc*. 2003;23:527–36.
- Widatallah HM, Johnson C, Berry FJ. The influence of ball milling and subsequent calcination on the formation of LiFeO<sub>2</sub>. *J Mater Sci*. 2002;37:4621–5.
- Kavanlooe M, Hashemi B, Maleki-Ghaleh H, Kavanlooe J. Effect of annealing on phase evolution, microstructure, and magnetic properties of nanocrystalline ball-milled LiZnTi ferrite. *J Electron Mater*. 2012;41:3082–6.
- Gee SH, Hong YK, Park MH, Erickson DW, Lamb PJ. Synthesis of nanosized (Li<sub>0.5x</sub>Fe<sub>0.5x</sub>Zn<sub>1-x</sub>)Fe<sub>2</sub>O<sub>4</sub> particles and magnetic properties. *J Appl Phys*. 2002;91:7586–8.
- Widatallah HM, Ren XL, Al-Omari IA. The influence of TiO<sub>2</sub> polymorph, mechanical milling and subsequent sintering on the formation of Ti-substituted spinel-related Li<sub>0.5</sub>Fe<sub>2.5</sub>O<sub>4</sub>. *J Mater Sci*. 2006;41:6333–8.
- Surzhikov AP, Lysenko EN, Malyshev AV, Pritulov AM, Kazakovskaya OG. Influence of mechanical activation of initial reagents on synthesis of lithium ferrite. *Russ Phys J*. 2012;6:672–7.
- Surzhikov AP, Lysenko EN, Vlasov VA, Malyshev AV, Nikolaev EV. Thermal analysis study of solid-phase synthesis of zinc- and

- titanium-substituted lithium ferrites from mechanically activated reagents. *J Therm Anal Calorim.* 2015;122:1347–53.
22. Brown ME, Dollimore D, Gallway AK. Reaction in solid state. *Comprehensive chemical kinetics.* Amsterdam: Elsevier; 1980.
  23. Opfermann J. Kinetic analysis using multivariate non-linear regression. *J Therm Anal Calorim.* 2000;60:641–58.
  24. Moukhina E. Determination of kinetic mechanisms for reactions measured with thermoanalytical instruments. *J Therm Anal Calorim.* 2012;109:1203–14.
  25. Sharma P, Uniyal P. Investigating thermal and kinetic parameters of lithium titanate formation by solid-state method. *J Therm Anal Calorim.* 2017;128:875–82.
  26. Lysenko EN, Nikolaev EV, Surzhikov AP. TG study of the Li<sub>0.4</sub>Fe<sub>2.4</sub>Zn<sub>0.2</sub>O<sub>4</sub> ferrite synthesis. *IOP Conf Series. Mater Sci Eng.* 2016;110:012092.
  27. Friedman HL. Kinetics of thermal degradation of char-forming plastics from thermogravimetry. Application to a phenolic plastic. *J Polym Sci Part C.* 1964;6:183–95.